Chemical Science

ROYAL SOCIETY OF CHEMISTRY

EDGE ARTICLE

View Article Online
View Journal | View Issue

Cite this: *Chem. Sci.*, 2023, **14**, 10875

All publication charges for this article have been paid for by the Royal Society of Chemistry

Received 15th June 2023
Accepted 18th September 2023

DOI: 10.1039/d3sc03056c

rsc.li/chemical-science

Supramolecular alternating copolymers with highly efficient fluorescence resonance energy transfer†

Anwesha Chakraborty,[a] Pradipta Kumar Das,[b] Biman Jana *[b] and Suhrit Ghosh *[a]

This article reports alternating supramolecular copolymerization of two naphthalene-diimide (NDI)-derived building blocks (NDI-1 and NDI-2) under thermodynamic control. Both monomers contain a central NDI chromophore, attached to a hydrocarbon-chain and a carboxylic-acid group. The NDI core in NDI-2 is symmetrically substituted with two butane-thiol groups, which makes it distinct from NDI-1. In decane, a 1 : 1 mixture of NDI-1 and NDI-2 shows spontaneous gelation and a typical fibrillar network, unlike the behavior of either of the components individually. The solvent-dependent UV/vis spectrum of the mixed sample in decane shows bathochromically shifted sharp absorption bands and a sharp emission band (holds a mirror-image relationship) with a significantly small Stokes shift compared to those in $CHCl_3$, indicating J-aggregation. In contrast, the aggregated spectra of the individual monomers show broad structureless features, suggesting ill-defined aggregates. Cooling curves derived from the temperature-dependent UV/vis spectroscopy studies revealed early nucleation and a signature of well-defined cooperative polymerization for the mixed sample, unlike either of the individual components. Molecular dynamics simulations predicted the greatest dimer formation tendency for the NDI-1 + NDI-2 (1 : 1), followed by pure NDI-1 and NDI-2. Theoretical studies further revealed a partial positive charge in the NDI ring of NDI-1 when compared to NDI-2, promoting the alternating stacking propensity, which is also favored by the steric factor as NDI-2 is core-substituted with alkyl thiols. Such theoretical predictions fully corroborate with the experimental results showing 1 : 1 stoichiometry (from Job's plot) of the two monomers, indicating alternate stacking sequences in the H-bonded (syn–syn catemer type) supramolecular copolymer. Such alternating supramolecular copolymers showed highly efficient (>93%) fluorescence resonance energy transfer (FRET).

Introduction

Supramolecular polymerization has emerged as a powerful tool for the synthesis of diverse molecular assemblies with precise internal order and functional utility.[1] In the recent past the focus has been shifted to supramolecular copolymers,[2–7] which represent adaptive multicomponent systems with tuneable photophysical properties and density of surface-displayed functional groups, attractive for functions including supramolecular biomaterials,[4] catalysis,[5] light harvesting,[6] long range exciton transport[7] and others. Recent development in this field[2,3] helps in directly correlating supramolecular copolymerization with well-established covalent copolymerization in terms of the relationship between the reactivity ratio of the monomers and the nature of the copolymer, microstructure, and other structural aspects. By virtue of this, it has been possible to demonstrate synthesis of well-defined supramolecular blocks, alternating or statistical copolymers in the past few years, mostly from different organic π-systems.[2,3] In most of these recent examples, hydrogen-bonding functional groups (amides and others) are attached to a central π-system, and when two or more such monomers are allowed to copolymerize, it becomes essential (not sufficient) that H-bonding functional groups are properly placed in the adjacent dissimilar monomers, so that the aromatic interaction and H-bonding can operate in a synchronized manner, failing which segregated homo-polymerization may dominate.[7] Manifestation of such possibilities depends on the relative dimensions of the two (or more) π-systems, involved in the copolymerization, but such stringent structural requirements may not be satisfactory moving from one system to another. We envisaged that, instead of this common strategy in which both the H-bonding group and the π-system are part of the backbone, if the chromophores remain as pendants, then the H-bonded chain can propagate independently, allowing the pendant chromophores to organize

[a]*School of Applied and Interdisciplinary Sciences, Indian Association for the Cultivation of Science, 2A and 2B Raja S. C. Mullick Road, Kolkata, 700032, India. E-mail: psusg2@iacs.res.in*

[b]*School of Chemical Sciences, Indian Association for the Cultivation of Science, 2A and 2B Raja S. C. Mullick Road, 700032, Kolkata, India. E-mail: pcbj@iacs.res.in*

† Electronic supplementary information (ESI) available: Sample preparation, materials, methods, instrumental details, experimental details for supramolecular copolymerization, MD simulation details and additional figures. See DOI: https://doi.org/10.1039/d3sc03056c

freely in their favourable mode. To test such possibilities, we have explored supramolecular copolymerization of two carboxylic-acid appended naphthalene-diimide (NDI)-derived monomers, namely NDI-1 and NDI-2 (Fig. 1a). We had earlier reported NDI-1 and structurally similar derivatives,[8] in which extended H-bonding among the carboxylic acid groups in the syn–syn catemer motif produced 1D-supramolecular polymers, but not in pure form as other motifs of H-bonding between the carboxylic acid groups operate simultaneously. We have now introduced a second monomer NDI-2, which is structurally similar to NDI-1 except for the core-substitution,[9] by virtue of which it exhibits distinct optical properties which is useful for probing copolymerization by spectroscopy techniques. Furthermore, we have recently reported J-aggregation of amide-functionalized sulphur-substituted NDI derivatives,[10] with remarkably high fluorescence quantum yield, which prompted us to use sulphur-substituted NDI for supramolecular copolymerization. In this article we report cooperative supramolecular copolymerization between NDI-1 and NDI-2 under thermodynamic control and reflect on the copolymer structure and sequence and thermodynamic aspects using the experimental and molecular dynamics (MD) simulation results. Furthermore, we show fluorescence resonance energy transfer (FRET)[11] between NDI-1 and NDI-2 in the supramolecular copolymers with remarkably high efficiency that has been rarely reported in the literature.[6]

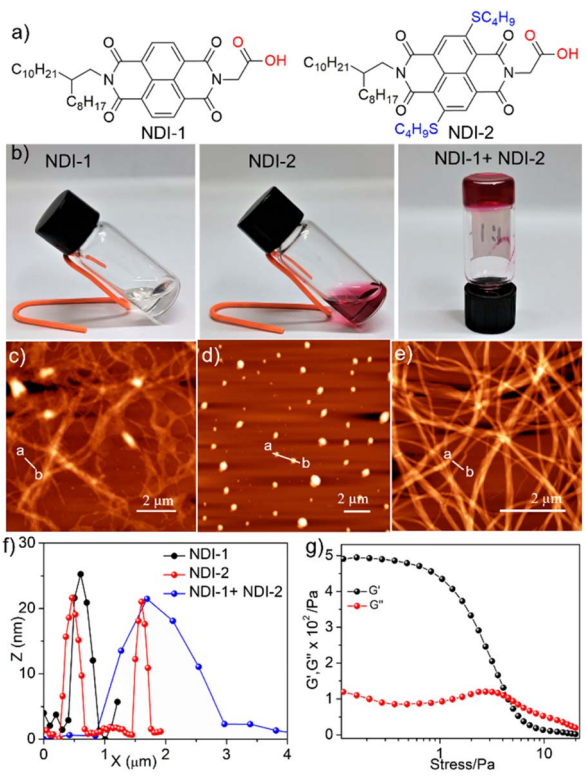

Fig. 1 (a) Structures of NDI-1 and NDI-2; (b) images of sol/gel of NDI-1, NDI-2 and NDI-1 + NDI-2 (1 : 1) in decane ($c = 4.0$ mM); AFM images of samples prepared from (c) NDI-1, (d) NDI-2 and (e) 1 : 1 mixture of NDI-1 + NDI-2 in decane ($c = 0.2$ mM); (f) height profiles along a–b in the images shown in (c–e); (g) stress amplitude sweep measurement data of the NDI-1 + NDI-2 (1 : 1) gel in decane ($c = 10.0$ mM).

Results and discussion

Supramolecular polymerization and copolymerization

Synthesis of NDI-1 was reported by us elsewhere.[8b] NDI-2 was prepared by multi-step synthesis (Scheme S1†) and isolated as a red solid with ~6% overall yield. Gelation[12] ability of the two NDI building blocks and their equimolar mixture was tested in decane. Neither NDI-1 nor NDI-2 produced a gel (Fig. 1b) in decane up to a concentration of 5.0 mM. In sharp contrast their 1 : 1 mixture spontaneously produced a transparent red gel (Fig. 1b) when the hot solution in decane was cooled to room temperature. The critical gelation concentration (CGC) and gel-to-sol transition temperature (T_g) of this mixed gel was estimated to be ~0.6 mM and ~80 °C ($c = 10$ mM), respectively. Rheological properties of the gel were checked by a stress-amplitude sweep measurement in which the variations of the storage modulus (G') and loss modulus (G'') were monitored as a function of applied stress (Fig. 1g). Initially G' (5000 Pa) was significantly larger than G'' (1200 Pa), as typically observed for a gel phase.[13] With increasing stress they remained almost invariant up to a critical point and then crossed each other, revealing the yield stress to be 4.5 Pa. Morphology was examined by atomic force microscopy (AFM) (Fig. 1c–e) with diluted gel/sol samples ($c = 0.2$ mM). The NDI-1 + NDI-2 (1 : 1) mixed gel showed entangled fibrillar morphology with the height of the thinnest fiber ~40 nm, while NDI-2 showed near spherical irregular particles (height ~20–30 nm). NDI-1, on the other hand, showed an irregular fibrillar structure as reported by us before due to the possible simultaneous formation of multiple aggregates by different H-bonding motifs of the carboxylic acid

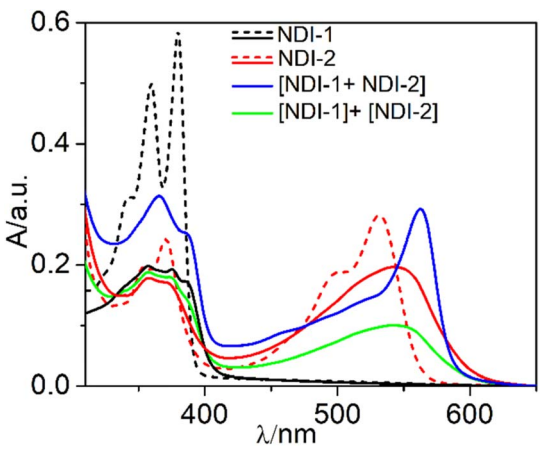

Fig. 2 UV/vis spectra of NDI-1, NDI-2 and NDI-1 + NDI-2 (1 : 1) in $CHCl_3$ (dashed line) or decane (solid line) [$T = 25$ °C, $l = 0.1$ cm]. The total monomer concentration was kept at 0.2 mM for all samples, which indicates that the concentration of NDI-1 or NDI-2 in the mixture is 0.1 mM. The green (solid) line represents mathematical summation of [aggregated spectra of NDI-1 (black solid line) + NDI-2 (red solid line)]/2 and is shown here to compare with the actual aggregated spectrum of the mixed sample (blue solid line).

group.[8] These results strongly suggest formation of supramolecular copolymers of NDI-1 and NDI-2 with the emergence of new physical properties, when compared to those of the individual monomers. This was clearly evident from the UV/vis spectroscopy studies (Fig. 2).

Monomeric spectra of both NDI-1 and NDI-2 in $CHCl_3$ show sharp absorption bands in the range of 300–400 nm and NDI-2 also exhibits an additional intra-molecular charge-transfer band in the window of 450–550 nm. In decane, both chromophores exhibit broad spectra with a concomitant reduction in the peak intensity, indicating aggregation. Interestingly, the UV/vis spectrum of NDI-1 + NDI-2 (1 : 1) in decane shows distinct features when compared to the aggregated spectra of the individual monomers. Especially noteworthy is the appearance of a sharp, bathochromically shifted (~30 nm) new charge-transfer band (λ_{max} = 562 nm), indicating J-aggregation[10,14] in the supramolecular copolymer. Overall, from the UV/vis data (Fig. 2) it is evident that the aggregated spectrum of NDI-1 + NDI-2 (1 : 1) in decane is totally different than the mathematical sum spectra of the aggregates of the two individual building blocks, which eliminates the possibility of formation of segregated homopolymers or supramolecular block copolymers; rather it strongly evokes the formation of supramolecular copolymers with either statistical or alternating sequences.

To get further insight into the supramolecular copolymerization, a hot solution of NDI-1 + NDI-2 (1 : 1) in decane (c = 0.2 mM) was cooled from 90 °C to 25 °C and the change in the absorbance spectrum was monitored as a function of temperature (Fig. 3a). At the highest temperature the spectrum appeared similar to that in $CHCl_3$ indicating a monomeric state. With decreasing temperature, the monomeric band (λ_{max} = 523 nm) started disappearing and *in lieu* the red-shifted J-aggregate band (λ_{max} = 561 nm) appeared gradually. The mole fraction of aggregate (α_{agg}) at each temperature was calculated from the absorption intensity of the J-band (λ_{max} = 561 nm) and plotted as a function of temperature (Fig. 3b). So the constructed cooling curve (Fig. 3b) showed a non-sigmoidal shape that is typically seen for cooperative supramolecular polymerization,[15,16] with an elongation temperature (T_e) of ~62 °C. Temperature-dependent UV/vis experiments were carried out for NDI-1 (Fig. S1†) and NDI-2 (Fig. S2†) under identical experimental conditions and cooling curves (Fig. 3) were constructed accordingly. In sharp contrast to the supramolecular copolymer, NDI-2 alone exhibited a peculiar cooling curve (Fig. 3), that neither indicates a cooperative nor isodesmic mechanism. Hence it can be concluded that NDI-2 lacks any well-defined supramolecular polymerization pathway; rather immiscibility driven irregular aggregation leads to the observed change in the UV/vis spectra. NDI-1, on the other hand, showed (Fig. 3) sluggish elongation at much lower temperature, which was studied in detail in our previous report[8] and can be attributed to its pathway complexity. By comparing these cooling curves, it is evident that the hetero-nucleation leads to a well-defined distinct supramolecular polymerization pathway with significantly greater propensity than the homo-nucleation for either of the two monomers in their homo-polymerization. To check the stability of the supramolecular copolymer,

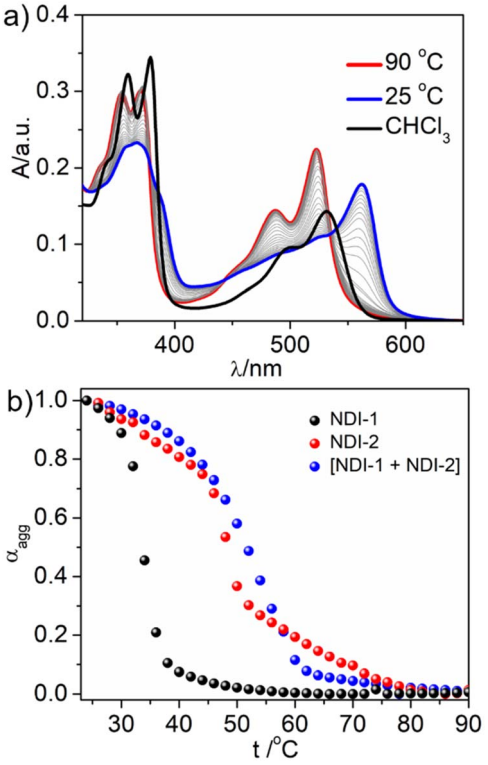

Fig. 3 (a) Variable temperature (from 90 °C to 25 °C at a rate of 2 °C min^{-1}) UV/vis spectra of NDI-1 + NDI-2 (1 : 1) in decane. For comparison the UV/vis spectrum in $CHCl_3$ at 25 °C is also shown in the plot. c = 0.2 mM and l = 0.1 cm; (b) variation of α_{agg} (estimated from change in intensity at 390 nm for NDI-1 and 561 nm for NDI-2 or the 1 : 1 mixture of NDI-1 + NDI-2) as a function of temperature.

variable temperature UV/vis spectra of NDI-1 + NDI-2 (1 : 1) were monitored as a function of temperature (Fig. 4a). With gradual heating, the J-band at 561 nm started reducing in intensity and *in lieu* the blue shifted monomeric band re-appeared (Fig. 4a) with other concomitant spectral changes suggesting reversible transformation into the monomeric state at elevated temperature. The melting curve (Fig. 4b) indicated α_{50} (T) to be ~60 °C. A consistent result was obtained in μ-DSC experiments (Fig. 4b), revealing a clear phase transition for the 1 : 1 gel in decane at ~55 °C. We further examined NDI-1/NDI-2 composition dependent thermal disassembly of the copolymers by variable temperature UV/vis spectroscopy. To our surprise we noticed almost identical melting curves (Fig. 4c) of the three representative mixed samples (NDI-1 : NDI-2 = 1 : 2, 1 : 1 or 2 : 1), constructed from the temperature dependent UV/vis spectra (Fig. S3†). Melting curves of the 1 : 1 sample at 1 °C min^{-1} and 2 °C min^{-1} were compared while similar results were found (Fig. 4c). Such identical melting curves for different compositions cannot be rationalized if they form a statistical copolymer, as in that case the composition of the copolymer would greatly vary depending on the ratio of the two monomers. Instead, these identical melting curves, irrespective of the monomer feed ratio, suggest the formation of the same alternating copolymer in all three cases. Melting curves for the three different mixed samples (NDI-2/NDI-1 = 1 : 1, 1 : 2 or 1 : 3) with

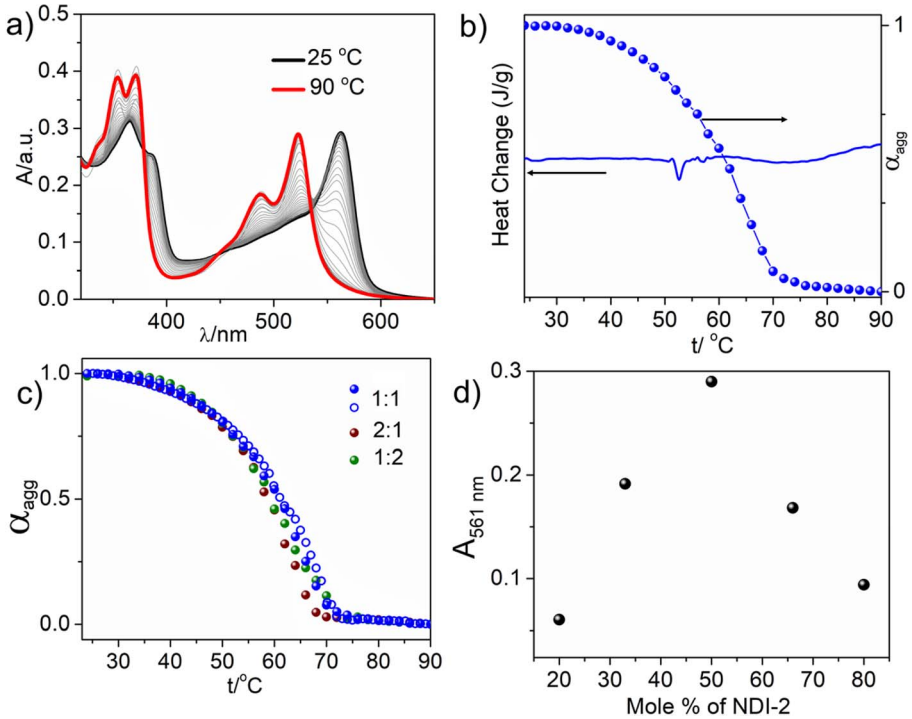

Fig. 4 (a) Temperature dependent (heating from 25 °C to 90 °C at a rate of 2 °C min^{-1}) UV/vis spectra of the 1 : 1 mixture of NDI-1 + NDI-2 in decane; (b) variation of α_{agg} (estimated from change in intensity at 561 nm for the 1 : 1 mixed sample along with a micro-DSC thermogram (heating) of the 1 : 1 gel in decane ($c = 5$ mM) showing disassembly in the similar temperature range. This melting curve, when compared with the cooling curve (Fig. 3b) of the same sample, reveals hysteresis, indicating that there could be pathway complexity in supramolecular polymerization; (c) variation of α_{agg} (calculated from change in intensity at 561 nm) as a function of temperature (heating from 25 °C to 90 °C, $c = 0.2$ mM) for the three mixed samples heated at a rate of 2 °C min^{-1} (filled circles) or at a rate of 1 °C min^{-1} (open circle) only for the 1 : 1 sample; (d) Job's plot for NDI-1 + NDI-2, constructed from the J-band (561 nm) intensity with different NDI-1/NDI-2 ratios (total concentration fixed at 0.2 mM).

a fixed NDI-2 concentration were compared (Fig. S4†). A similar melting pattern was observed but the transition temperatures as well as α_{50} (T) were slightly increased with an increasing amount of NDI-1 as the total solute concentration increased in samples with a stoichiometric imbalance. In μ-DSC experiments, two different phase transition temperatures were noticed for 1 : 2 (~39 °C and ~50 °C) and 2 : 1 (~47 °C and ~52 °C) gels (Fig S5†), indicating formation of alternating copolymers, along with a homopolymer of the excess component.

To examine this further, we probed the behaviour of NDI-1 + NDI-2 with varying compositions such as 1 : 4, 1 : 2, 1 : 1, 2 : 1 and 4 : 1, while the total monomer concentration was kept fixed. All five mixed samples showed spontaneous gelation in decane ($c = 2$ mM) (Fig. S6†). UV/vis spectra of the diluted gels showed (Fig. S7†) a characteristic sharp absorption band (λ_{max} ~561 nm) for all five samples, that has been specifically assigned to the copolymer. From these data, Job's plot was constructed, which showed (Fig. 4d) maximum intensity of the J-band for the 1 : 1 composition, strongly indicating an alternating stacking sequence of the two monomers in their supramolecular copolymers.[17] In this case, in the mixed samples with a stoichiometric imbalance of the two monomers (say 1 : 2 or 2 : 1 of NDI-1/NDI-2), the excess monomer should form additional homo-aggregates as they cannot be incorporated in the supramolecular copolymer with an alternating sequence. Indeed, the AFM images of the NDI-1 + NDI-2 (1 : 2) sample showed a significant presence of spherical particles (Fig. S8†), similar to the homo-aggregate of NDI-2 (Fig. 2), in addition to the entangled fibrils of the alternating supramolecular copolymer. Thinking in a similar line one would expect to observe the presence of the homopolymer of NDI-1 along with the supramolecular copolymer in the mixed sample with excess NDI-1 (NDI-1/NDI-2 = 3 : 1). But this was difficult to identify in the AFM image (Fig. S9†) because the NDI-1 homopolymer too exhibits fibrillar morphology.[18]

Fluorescence resonance energy transfer (FRET)

Next, we examined fluorescence properties of the alternating supramolecular copolymer and compared them with those of NDI-2 (Fig. 5a). For the 1 : 1 supramolecular copolymer in decane, a sharp emission band was noticed (Fig. 5a) which holds a mirror-image relationship with the absorption band. Emission intensity was significantly higher compared to that of monomeric NDI-2 in $CHCl_3$ (Fig. 5b), indicating enhanced emission because of J-aggregation, which is consistent with our previous report on the J-aggregation of a structurally different sulphur-substituted NDI gelator.[10] Furthermore, a significantly smaller Stokes shift (22 nm) in the aggregated state compared to that in the monomeric state (35 nm) was noticed (Fig. 5a) which is considered a typical signature of J-aggregation.[14]

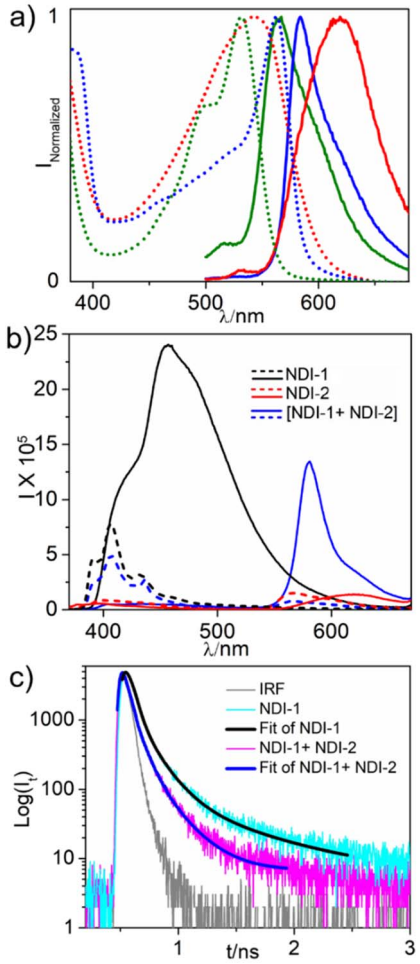

Fig. 5 (a) Intensity normalized absorption (dotted line) and emission (solid line) of NDI-2 in the presence (blue) and absence of NDI-1 (red) in decane and in $CHCl_3$ (green) when excited at 480 nm; (b) emission spectra of NDI-1 and NDI-2 and their 1 : 1 mixture in the monomeric ($CHCl_3$, dashed line) state and in aggregated state in decane (solid line) (λ_{ex} = 360 nm) (c) fluorescence transients of NDI-1 in the presence (blue) and absence of NDI-2 (black) (λ_{ex} = 360 nm, λ_{em} = 430 nm, slit-3 nm, and c = 0.2 mM).

Interestingly, the homo-aggregate of NDI-2 showed (Fig. 5a) a broad, less intense emission with a large Stokes shift (75 nm), further confirming distinct photophysical properties of the same dye in the supramolecular copolymer. Now the excitation wavelength was changed to 360 nm where the aggregated band appeared for NDI-1. A broad emission band in the window of ~400–600 nm was noticed (Fig. 5b) that is quite different than the monomeric emission in $CHCl_3$. This issue was deliberated in detail in our previous work[8a] and assigned to simultaneous formation of multiple aggregates due to pathway complexity, which has been examined in more detail by us in a recent report.[8b]

Now considering a significant overlap between the emission spectra of NDI-1 and absorption spectra of NDI-2 (when both are in the aggregated state in decane) (Fig. S10a†), FRET was anticipated in the supramolecular copolymer, which is ubiquitous in natural light harvesting systems. Despite many reports showing such energy transfer in synthetic supramolecular systems,[6,19] it is imperative to have a highly ordered organization of the donor and acceptor chromophores to realize highly efficient energy transfer. Now for the alternating supramolecular copolymer, with the same 360 nm excitation, the emission band for the NDI-1 aggregate was almost quenched and *in lieu* a sharp emission band appeared corresponding to the J-aggregate of NDI-2 which is identical to that obtained by 480 nm excitation (Fig. 5b). However, no such emission band was noticed for the NDI-homopolymer for the 360 nm excitation that eliminates any significant contribution from the direct excitation of NDI-2 (or any other factor) and strongly suggests FRET from the NDI-1 donor to the NDI-2 acceptor when they are co-located in the alternating supramolecular copolymer. This was further evident from the TCSPC studies that showed (Fig. 5c) that fluorescence transients of NDI-1 (donor) decay at a significantly faster rate in the presence of NDI-2 (acceptor), indicating nonradiative resonance type energy transfer between NDI-1 and NDI-2. The average lifetime of NDI-1 was found to be 0.03 ns in the presence of NDI-2 which is significantly less than that of NDI-1 (0.46 ns) in the absence of NDI-2. Energy transfer efficiency was estimated to be ~98% from the steady state fluorescence spectra, while ~93% from the TCSPC studies. Such high values, rarely reported in the literature, indicate that the present alternating supramolecular copolymer can be considered a highly promising scaffold for light harvesting. The rate of energy transfer was estimated to be 28 ns^{-1} (see the ESI† for details). Furthermore, for the 1 : 1 sample, a sharp and distinct emission band was noticed (Fig. S11†), which further supports alternating copolymerization and the absence of any homopolymer of either NDI-1 or NDI-2.

Molecular dynamics (MD) simulations

The internal order, sequence and thermodynamics of supramolecular copolymers and origin of the alternating stacking mode were further examined by theoretical studies. To gain molecular insight regarding this copolymerization behaviour, all-atom molecular dynamics simulations of NDI-1, NDI-2, and their 1 : 1 mixture in decane were performed. Automated Topology Builder (ATB version 3.0) was used to obtain a suitable structure and forcefield parameters of these molecules.[20,21]

GROMACS 2020.6 was used along with a modified gromos54a7 forcefield to perform and analyse MD simulations.[22] We have also used VMD[23] and PYMOL to visualize and analyse the structures and trajectories obtained from the performed MD simulations.

All the details of the system preparation and MD simulation along with the analysis are included in the ESI.† At first, we took a total of 40 molecules to prepare 3 systems (40 NDI-1, 40 NDI-2, and 20 : 20 NDI-1 and NDI-2). NDI-1 and NDI-2 both have an end-to-end distance of ~2.1 nm in their fully extended states, calculated from the carboxyl group to the end of the branched chains. All the systems were solvated in decane and properly equilibrated in both NVT and NPT ensembles. During the production run, in all the systems, we observed the formation of different sized oligomers. We took the most stable dimer from

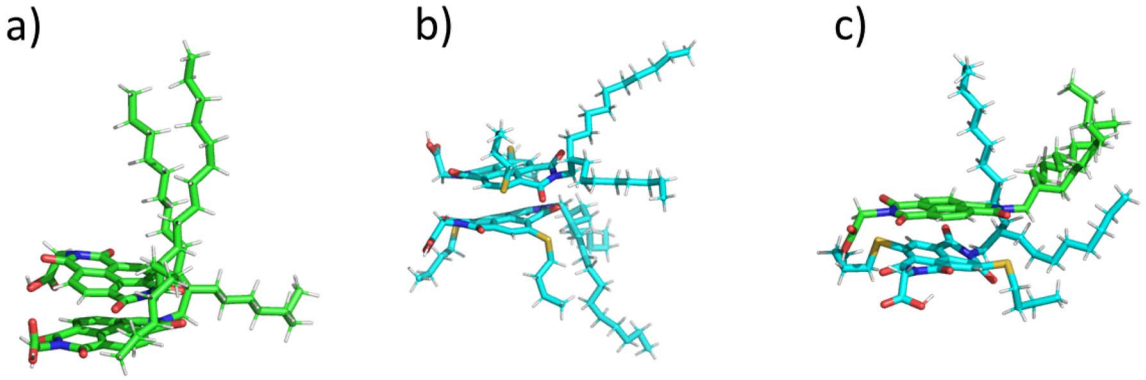

Fig. 6 Pair formation for each system. (a) Pair between 2 NDI-1; (b) pair between 2 NDI-2; (c) pair between NDI-1 and NDI-2.

each system and constructed a rough binding free energy surface using the umbrella sampling method with the distance between the dimers as the pulling coordinate to obtain the dimer from their individual minima (Fig. 6). These dimers are then used to estimate their stability by evaluating the binding free energy in terms of potential of mean force (PMF) using the umbrella sampling method with the distance between the central rings of the dimers as a pulling coordinate. The free energy was calculated by keeping one of the NDI rings restrained and the distance was varied for the other ring. The free energy was set to be 0 at 1 nm distance to get the idea of relative stability among all 3 dimers. It was evident from the minima of the free energy profiles (Fig. 7) that 1 : 1 NDI-1 + NDI-2 has a greater dimer formation tendency than both pure NDI-1 and NDI-2 systems. NDI-2 is least biased towards dimer formation and NDI-1 stands in between these two scenarios. The minimum in free energy of the NDI-1-NDI-2 dimer is around -32 kJ mol^{-1}, whereas NDI-1 and NDI-2 have their minimum at -25 kJ mol^{-1} and -17 kJ mol^{-1}, respectively. The lack of a deeper minimum in the case of NDI-2 compared to the rest suggests its reluctance towards forming any stable dimer. Also, the gradual shift of the minima corresponding to each PMF towards larger distances in the order of NDI-1, NDI-1 + NDI-2, and NDI-2 implies that the bulkier side chain of NDI-2 is directly associated with the compactness of the dimer (Fig. 7).

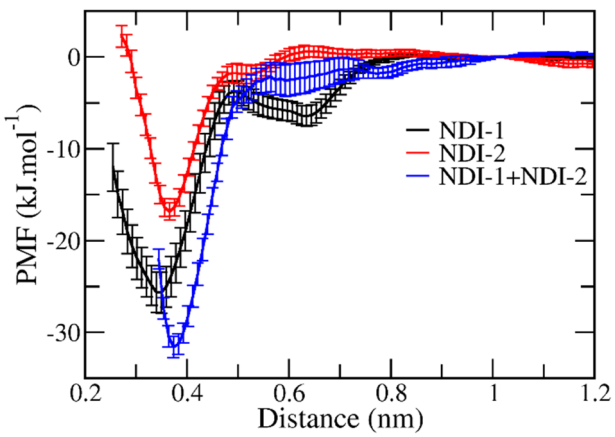

Fig. 7 Potential of mean force (PMF) of the dimers formed, NDI-1, NDI-2 and NDI-1 + NDI-2 (1 : 1).

We also inspected the stability of trimers (Fig. S12†) formed during the production run of the mixed system, and we observed that the NDI-1 and NDI-2 interface is more stable than the NDI-1 and NDI-1 interface (Fig. S13†). A close inspection of the dimer configurations suggests that the bulky hydrophobic groups stay on one side of the dimer while the hydrogen bonding groups are on the other side. We calculated electrostatic potential on the surfaces of NDI-1 and NDI-2 using the Gaussian package (Gaussian09). Our observations indicate the presence of charge differences in NDI-1 and NDI-2 relative to each other. NDI-1 is partially positively charged on the main NDI ring relative to NDI-2 which is relatively less positive compared to NDI-1, which is conceivable considering the core substitution in NDI-2. This charge difference may play a crucial role in stacking efficiency of the mixed system (Fig. S14†).

We have also been able to identify the larger motif at work behind this efficient copolymerization using all-atom molecular dynamics simulations. For the NDI-1 system, we observed several well-organized NDI-1 oligomers stacking, accommodating around 5 to 8 NDI-1 in each stack (Fig. 8a). Here also, we find that the hydrophobic side chains stay on one side of the stacking while the carboxylic groups stay on the other side. Then, two such stacked clusters come together to form intercluster h-bonds in a zig-zag manner, which was proposed in our previous report.[8] This situation is mostly steered by the bulky sidechain orientations on one side which allow the hydrogen bonding partners from different stacked clusters to face each other. A more organized stacking through hydrogen bonds was modelled based on this motif for both homogeneous (NDI-1 oligomers) (Fig. 8b) as well as alternate (NDI-1 + NDI-2 oligomers) stacking clusters (Fig. 8c). It is noteworthy that such open chain H-bonding in the syn–syn catemer motif was supported by FT-IR studies (Fig. S16†).[24] Furthermore the structure of the supramolecular copolymer (Fig. 8c) was also supported by powder X-ray diffraction studies (Fig. S17†) which showed a sharp peak ($2\theta = 2.62°$) corresponding to a $d = 34$ Å, which matches with the estimated width of the column (38 Å from MD simulations) consisting of two NDI monomers. In fact, a similar sharp peak with a slightly different d value (30 Å) was

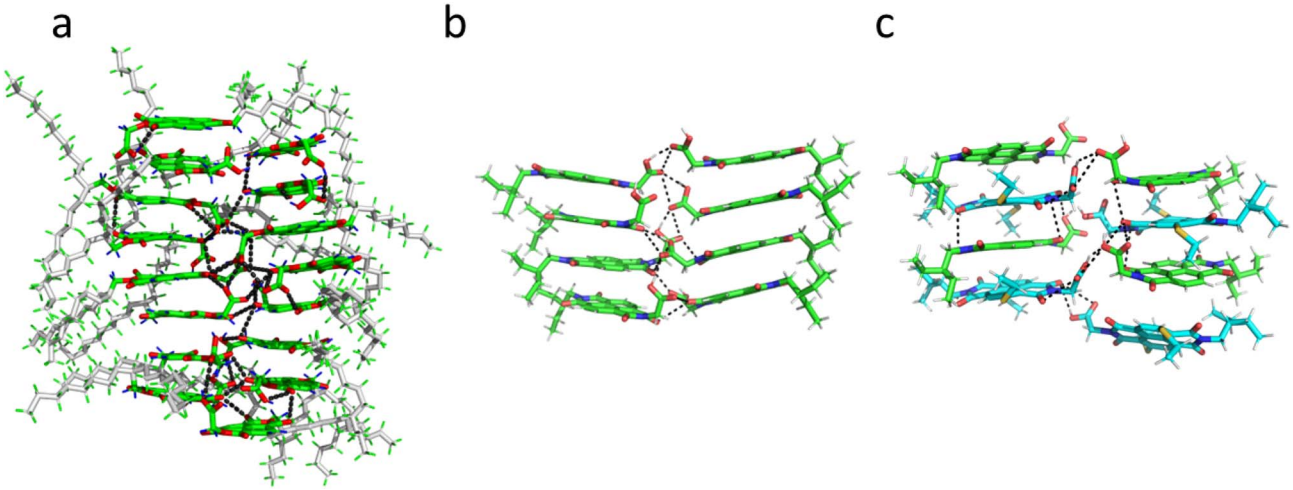

Fig. 8 (a) NDI-1 cluster, black lines indicating hydrogen bonds between carboxylic acid groups; (b) NDI-1 modelled hydrogen bond motif between two stacked clusters; the inter-cluster hydrogen bond pattern is clearly visible in a zig-zag manner; (c) NDI-1 + NDI-2 inter-cluster hydrogen bonds retaining a similar motif modelled in the NDI-1 system.

also obtained for NDI-1, but not for NDI-2, which corroborates with the MD simulation results suggesting a weak supramolecular polymerization propensity of NDI-2. Therefore, our MD simulations suggest that alternate stacking-based oligomerization followed by hydrogen bonding based association of the stacked oligomers results in fibrilization, which fully corroborate with the experimental results.

Conclusions

Overall, in this manuscript we have shown alternating supramolecular copolymerization of two carboxylic-acid functionalized NDI derivatives (NDI-1 and NDI-2), which differ by the thiol substitution in the NDI core of NDI-2. Due to the possibility of multiple H-bonding motifs (open chain with parallel/antiparallel orientation, dimers and others) of the carboxylic-acid group as well as other electronic and/or steric factors, neither NDI-1 nor NDI-2 individually is capable of adopting a specific supramolecular polymerization pathway. In sharp contrast, their 1 : 1 mixture shows typical cooperative supramolecular polymerization, leading to well-defined J-aggregation and gelation in decane, unlike either NDI-1 or NDI-2. Based on experimental and MD-simulation studies, it is evident that these two monomers copolymerize by open-chain H-bonding (zig-zag fashion) with alternating stacking sequences that is favoured by both electronic and steric factors. Basically, thiol substitution makes the NDI-2 ring relatively more electron rich than NDI-1 and imparts steric constraints, both of which favour hetero-nucleation and alternate stacking, reminiscent of the reactivity ratio-based principle for alternate covalent copolymerization. Such a well-defined alternating supramolecular copolymer exhibits FRET with near quantitative efficiency that has been rarely reported in the literature. Despite recent progress in the field, only a handful of examples are known for supramolecular copolymerization under thermodynamic control and most of those designs are system-specific. In this sense the present molecular design is not only simple, but importantly the H-bonding chain formation is decoupled from the π-stacking, which in principle should allow expanding the scope for supramolecular copolymerization with diverse π-systems (with 2 or more monomers) under thermodynamic control for realizing new functional properties such as micropower energy harvesting, ferroelectricity, photothermal effect, cascade energy transfer and others by fine tuning the structure of the monomers, their internal order in the supramolecular copolymer or chirality. Such efforts are underway in our laboratory.

Data availability

Data generated during this study are available from the authors on reasonable request.

Author contributions

AC synthesized the molecules, carried out self-assembly studies and analyzed related data under the supervision of SG. PKD carried out MD simulation stuides and analyzed the data under the supervision of BJ. SG conceptulized the research problem. All authors contributed in manuscript writing and data analysis. Funding was generated by SG and BJ.

Conflicts of interest

There are no conflicts to declare.

Acknowledgements

AC thanks the DST Inspire program and IACS for a research fellowship. SG thanks the SERB for funding (Grant No: CRG/2020/002395). BJ thanks the SERB for funding (Grant No: CRG/2020/000756).

Notes and references

1 (*a*) F. J. M. Hoeben, P. Jonkheijm, E. W. Meijer and A. P. H. J. Schenning, *Chem. Rev.*, 2005, **105**, 1491; (*b*) M. Wehner and F. Würthner, *Nat. Rev. Chem*, 2020, **4**, 38; (*c*) R. D. Mukhopadhyay and A. Ajayaghosh, *Science*, 2015, **349**, 241; (*d*) J. Matern, Y. Dorca, L. Sánchez and G. Fernández, *Angew. Chem., Int. Ed.*, 2019, **58**, 16730; (*e*) S. Datta, S. Takahashi and S. Yagai, *Acc. Mater. Res.*, 2022, **3**, 259; (*f*) L. Yang, X. Tan, Z. Wang and X. Zhang, *Chem. Rev.*, 2015, **115**, 7196; (*g*) G. Ghosh, P. Dey and S. Ghosh, *Chem. Commun.*, 2020, **56**, 6757; (*h*) M. Hartlieb, E. D. H. Mansfield and S. Perrier, *Polym. Chem.*, 2020, **11**, 1083.

2 B. Adelizzi, N. J. Van Zee, L. N. J. de Windt, A. R. A. Palmans and E. W. Meijer, *J. Am. Chem. Soc.*, 2019, **141**, 6110.

3 (*a*) W. Wagner, M. Wehner, V. Stepanenko and F. Würthner, *J. Am. Chem. Soc.*, 2019, **141**, 12044; (*b*) A. Sarkar, R. Sasmal, C. Empereur-mot, D. Bochicchio, S. V. K. Kompella, K. Sharma, S. Dhiman, B. Sundaram, S. S. Agasti, G. M. Pavan and S. J. George, *J. Am. Chem. Soc.*, 2020, **142**, 7606; (*c*) P. Khanra, A. K. Singh, L. Roy and A. Das, *J. Am. Chem. Soc.*, 2023, **145**, 5270; (*d*) D. Görl, X. Zhang, V. Stepanenko and F. Würthner, *Nat. Commun.*, 2015, **6**, 7009; (*e*) B. Adelizzi, A. Aloi, A. J. Markvoort, H. M. M. Ten Eikelder, I. K. Voets, A. R. A. Palmans and E. W. Meijer, *J. Am. Chem. Soc.*, 2018, **140**, 7168; (*f*) P. Ahlers, K. Fischer, D. Spitzer and P. Besenius, *Macromolecules*, 2017, **50**, 7712; (*g*) H. Frisch, J. P. Unsleber, D. Lüdeker, M. Peterlechner, G. Brunklaus, M. Waller and P. Besenius, *Angew. Chem., Int. Ed.*, 2013, **52**, 10097; (*h*) S. H. Jung, D. Bochicchio, G. M. Pavan, M. Takeuchi and K. Sugiyasu, *J. Am. Chem. Soc.*, 2018, **140**, 10570; (*i*) W. Zhang, W. Jin, T. Fukushima, A. Saeki, S. Seki and T. Aida, *Science*, 2011, **334**, 340; (*j*) A. Das, G. Vantomme, A. J. Markvoort, H. M. M. ten Eikelder, M. Garcia-Iglesias, A. R. A. Palmans and E. W. Meijer, *J. Am. Chem. Soc.*, 2017, **139**, 7036; (*k*) L. N. J. de Windt, C. Kulkarni, H. M. M. ten Eikelder, A. J. Markvoort, E. W. Meijer and A. R. A. Palmans, *Macromolecules*, 2019, **52**, 7430; (*l*) S. Chakraborty, H. Kar, A. Sikder and S. Ghosh, *Chem. Sci.*, 2017, **8**, 1040; (*m*) S. Takahashi and S. Yagai, *J. Am. Chem. Soc.*, 2022, **144**, 13374; (*n*) L. Aratsu, R. Takeya, B. R. Pauw, M. J. Hollamby, Y. Kitamoto, N. Shimizu, H. Takagi, R. Haruki, S. Adachi and S. Yagai, *Nat. Commun.*, 2020, **11**, 1623; (*o*) J. Matern, Z. Fernandez and G. Fernandez, *Chem. Commun.*, 2022, **58**, 12309; (*p*) Y. Dorca, C. Naranjo, G. Ghosh, B. Soberats, J. Calbo, E. Ortí, G. Fernández and L. Sánchez, *Chem. Sci.*, 2022, **13**, 81.

4 (*a*) M. J. Webber, E. A. Appel, E. W. Meijer and R. Langer, *Nat. Mater.*, 2016, **15**, 13; (*b*) T. Liu, L. van den Berk, J. A. J. Wondergem, C. Tong, M. C. Kwakernaak, B. Ter Braak, D. Heinrich, B. van de Water and R. E. Kieltyka, *Adv. Healthcare Mater.*, 2021, **10**, 2001903; (*c*) S. Chakraborty, R. Khamrui and S. Ghosh, *Chem. Sci.*, 2021, **12**, 1101; (*d*) L. Albertazzia, F. J. Martinez-Veracoecheab, C. M. A. Leendersa, I. K. Voetsa, D. Frenkelb and E. W. Meijer, *Proc. Natl. Acad. Sci. U.S.A.*, 2013, **110**, 12203.

5 L. N. Neumann, M. B. Baker, C. M. A. Leenders, I. K. Voets, R. P. M. Lafleur, A. R. A. Palmans and E. W. Meijer, *Org. Biomol. Chem.*, 2015, **13**, 7711.

6 (*a*) A. Sarkar, T. Behera, R. Sasmal, R. Capelli, C. Empereur-mot, J. Mahato, S. S. Agasti, G. M. Pavan, A. Chowdhury and S. J. George, *J. Am. Chem. Soc.*, 2020, **142**, 11528; (*b*) Y. Han, X. Zhang, Z. Ge, Z. Gao, R. Liao and F. Wang, *Nat. Commun.*, 2022, **13**, 3546; (*c*) R. Liao, F. Wang, Y. Guo, Y. Han and F. Wang, *J. Am. Chem. Soc.*, 2022, **144**, 9775; (*d*) Q. Song, S. Goia, J. Yang, S. C. L. Hall, M. Staniforth, V. G. Stavros and S. Perrier, *J. Am. Chem. Soc.*, 2021, **143**, 382.

7 X. Jin, M. B. Price, J. R. Finnegan, C. E. Boott, J. M. Richter, A. Rao, S. M. Menke, R. H. Friend, G. R. Whittell and I. Manners, *Science*, 2018, **360**, 897.

8 (*a*) M. R. Molla, D. Gehrig, L. Roy, V. Kamm, A. Paul, F. Laquai and S. Ghosh, *Chem.–Eur. J.*, 2014, **20**, 760; (*b*) A. Chakraborty, R. Manna, A. Paul and S. Ghosh, *Chem.–Eur. J.*, 2021, **27**, 11458.

9 N. Sakai, J. Mareda, E. Vauthey and S. Matile, *Chem. Commun.*, 2010, **46**, 4225.

10 H. Kar and S. Ghosh, *Chem. Commun.*, 2016, **52**, 8818.

11 P. Rajdev and S. Ghosh, *J. Phys. Chem. B*, 2019, **123**, 327.

12 (*a*) S. Banerjee, R. K. Das and U. Maitra, *J. Mater. Chem.*, 2009, **19**, 6649; (*b*) S. S. Babu, V. K. Praveen and A. Ajayaghosh, *Chem. Rev.*, 2014, **4**, 1973.

13 (*a*) D. L. Blair, in *Molecular Gels: Structure and Dynamics*, ed. R. G. Weiss, RSC, 2018, ch. 2; (*b*) F. M. Menger and A. V. Peresypkin, *J. Am. Chem. Soc.*, 2003, **125**, 5340–5345.

14 F. Würthner, T. E. Kaiser and C. R. Saha-Möller, *Angew. Chem., Int. Ed.*, 2011, **50**, 3376.

15 C. Rest, R. Kandanelli and G. Fernández, *Chem. Soc. Rev.*, 2015, **44**, 2543.

16 M. M. J. Smulders, M. M. L. Nieuwenhuizen, T. F. A. de Greef, P. van der Schoot, A. P. H. J. Schenning and E. W. Meijer, *Chem.–Eur. J.*, 2010, **16**, 362.

17 S. Ghosh and S. Ramakrishnan, *Angew. Chem., Int. Ed.*, 2005, **34**, 5441.

18 In fact, in this case one cannot eliminate the possibility of the NDI-1 polymer growing from the supramolecular copolymer as NDI-1 too showed a well-defined polymerization pathway. This would lead to an interesting block structure consisting of an alternating copolymer of NDI-1 and NDI-2 as the first block and a homopolymer of NDI-1 as the second block. This will be studied in detail in the future.

19 V. K. Praveen, C. Ranjith, E. Bandini, A. Ajayaghosh and N. Armaroli, *Chem. Soc. Rev.*, 2014, **43**, 4222.

20 A. K. Malde, L. Zuo, M. Breeze, M. Stroet, D. Poger, P. C. Nair, C. Oostenbrink and A. E. Mark, *J. Chem. Theory Comput.*, 2011, **7**, 4026.

21 M. Stroet, B. Caron, K. M. Visscher, D. P. Geerke, A. K. Malde and A. E. Mark, *J. Chem. Theory Comput.*, 2018, **14**, 5834.

22 N. Schmid, A. P. Eichenberger, A. Choutko, S. Riniker, M. Winger, A. E. Mark and W. F. van Gunsteren, *Eur. Biophys. J.*, 2011, **40**, 843.

23 W. Humphrey, A. Dalke and K. Schulten, *J. Mol. Graphics*, 1996, **14**, 33.

24 H-bonding between the carboxylic acid groups in the homopolymers and copolymers was probed by FT-IR spectroscopy (Fig. S16†). In $CHCl_3$, a single peak at 3054 cm^{-1} was noticed for all three samples (NDI-1, NDI-2 or NDI-1 + NDI-2), which can be assigned to the O-H stretching of the free acid. In decane, this band shifted to lower frequency due to H-bonding. For homopolymers of NDI-1 and NDI-2, one major peak was observed at 2985 cm^{-1} and 3048 cm^{-1}, respectively, while that for the copolymer (1 : 1 NDI-1 + NDI-2) appeared at 3019 cm^{-1}, suggesting distinct H-bonding in the copolymer compared to the homopolymers, which is conceivable considering the overall structural difference of the copolymer compared to either of the homopolymers.